Experimental Neurology 318 (2019) 244–250

Contents lists available at ScienceDirect

Experimental Neurology

journal homepage: www.elsevier.com/locate/yexnr

Research Article

Deferoxamine therapy reduces brain hemin accumulation after intracerebral hemorrhage in piglets

Shengli Hu[a,b], Ya Hua[a], Richard F. Keep[a], Hua Feng[b], Guohua Xi[a,*]

[a] Department of Neurosurgery, University of Michigan, Ann Arbor, MI 48109, USA
[b] Department of Neurosurgery, Southwest Hospital, Chongqing 400038, China

ARTICLE INFO

Keywords:
Intracerebral hemorrhage
Deferoxamine
Hemin
Hemopexin
CD91
Swine

ABSTRACT

Hemopexin (Hpx) is critical for hemin scavenging after the erythrocyte lysis that occurs following intracerebral hemorrhage (ICH). Low-density lipoprotein receptor-related protein-1 (LRP1, also called CD91) is an important receptor through which the hemin-Hpx complex can undergo endocytosis. This study investigated changes in the hemin-Hpx-CD91 axis in both hematoma and perihematomal tissue in a large animal ICH model. The effect of deferoxamine (DFX) on hemin-Hpx-CD91 was also examined.

The study consisted of two parts. First, piglets had an injection of autologous blood into the right frontal lobe of brain and were euthanized from day 1 to day 7. Hematoma and perihematomal tissue of brains were used for hemin assay, immunohistochemistry, and immunofluorescence. Second, piglets with ICH were treated with deferoxamine or vehicle, and were euthanized for hemin measurement and Hpx and CD91 immunohistochemistry.

We found that there was an increase of hemin levels within the hematoma and perihematomal brain tissue after ICH. Hpx and CD91-positive cells were present in the clot and perihematomal tissue from day 1. Hpx and CD91 positive cells were Iba1 positive. After DFX therapy, hemin dropped markedly in the hematoma and perihematomal brain tissue. Furthermore, DFX treatment decreased the number of Hpx and CD91 positive cells in and around the hematoma.

In conclusion, hemin accumulation occurs in and around the hematoma. Increases in Hpx and CD91 may be important in scavenging that hemin. DFX treatment decreased hemin release from the hematoma and reduced the expression of Hpx and CD91.

1. Introduction

Intracerebral hemorrhage (ICH) is a particularly devastating form of stroke which causes severe clinical disability and mortality (Mendelow et al., 2013; Keep et al., 2012; Selim and Sheth, 2015; Schlunk and Greenberg, 2015). Clot resolution is an important pathophysiological process following ICH(Wilkinson et al., 2018). However, it can release toxic molecules such as hemoglobin and its degradation products, including hemin (Fe^{3+} protoporphyrin IX) and iron (Xi et al., 2006). Hemin is a toxic alarmin that can initiate oxidative stress, inflammation, cytotoxicity and brain parenchyma damage (Soares and Bozza, 2016; Wagener et al., 2001; Wang et al., 2016; Robinson et al., 2009). Thus, it is important to understand how extracellular hemin is removed after ICH. Hemopexin (Hpx) shows the highest known binding affinity for hemin ($Kd < 10^{-13}$ M), making hemin oxidatively inert(Schaer et al., 2013) and Hpx has protective effects in plasma and brain (Schaer et al., 2013; Aronowski and Zhao, 2011; Ascenzi et al., 2005). Moreover, recent studies demonstrated that Hpx possesses a pivotal ability in neuroprotection after hemorrhagic and ischemic stroke (Robinson et al., 2009; Ma et al., 2016; Dong et al., 2013; Chen et al., 2011). However, the changes in brain hemin and hemopexin following ICH are poorly understood.

Low-density lipoprotein receptor-related protein-1 (LRP1, also called CD91) is a transmembrane protein. As well as being a signaling receptor, it has versatile functions including protein scavenging and lipid endocytosis (Ramanathan et al., 2015; Lillis et al., 2008), and it has been identified as the receptor for hemin-Hpx complex endocytosis (Robinson et al., 2009; Schaer et al., 2013; Hvidberg et al., 2005). After cell uptake, the hemin-Hpx complex is dissociated in lysosomes and the hemin catabolized by heme oxygenase into biliverdin, carbon monoxide, and iron (Robinson et al., 2009; Schaer et al., 2013; Kumar and Bandyopadhyay, 2005; Piccard et al., 2007). Thus, CD91 has a key role

* Corresponding author at: R5018, BSRB, Department of Neurosurgery, University of Michigan, 109 Zina Pitcher Place, Ann Arbor, MI 48109-2200, USA.
E-mail address: guohuaxi@umich.edu (G. Xi).

https://doi.org/10.1016/j.expneurol.2019.05.003
Received 23 January 2019; Received in revised form 9 April 2019; Accepted 7 May 2019
Available online 10 May 2019
0014-4886/

in clearing free hemin to prevent toxicity.

Deferoxamine (DFX), an iron chelator, has been demonstrated to reduce hemorrhagic brain injury in animal models(Keep et al., 2012; Xi et al., 2006). In a swine ICH model, DFX significantly attenuated perihematomal iron accumulation, white matter injury and neuronal death (Gu et al., 2009; Xie et al., 2014). Recently, we found that DFX also slows hematoma lysis after ICH in aged rats (Hatakeyama et al., 2013). This was confirmed in another study, which showed that DFX reduced the formation of membrane attack complex and heme oxygenase-1 (HO-1) positive cells in hematoma after ICH in piglets (Cao et al., 2016).

The current study was to examine the expression of hemin, Hpx and CD91 in a piglet ICH model. The effect of DFX on those changes was also investigated.

2. Materials and methods

2.1. Animal preparation

All the animal studies were approved by the University of Michigan Committee on the Use and Care of Animals and performed according to the National Institutes of Health *Guide for the Care and Use of Laboratory Animals*. Male piglets weighing between 8 and 10 kg (Michigan State University, East Lansing) were used in the present study. Piglets were allowed free access to food and water before and after the surgical procedures. This study complies with the ARRIVE guidelines for reporting in vivo experiments. Randomization was carried out using odd/even numbers.

2.2. Surgical procedures

The ICH models were performed based on the technique as previously described (Xie et al., 2014; Cao et al., 2016; Zhou et al., 2014). Briefly, ketamine (25 mg/kg, i.m.) were used for sedation and 2% isoflurane were used through nose cone for anesthetization. The maintenance concentration of isoflurane was at 1.0 to 1.5% during the surgical operations. Core body temperature was kept at 37.5 ± 0.5 °C using a heating pad. A polyethylene catheter (PE-160) was inserted into the right femoral artery to obtain blood for brain injection and monitoring of arterial blood pressure, blood gases, and glucose during the surgery. A cranial burr hole (1.5 mm) located at the point 11 mm right of the sagittal suture and 11 mm anterior to the coronal suture was drilled. An 18-mm-long 20-gauge sterile plastic catheter was inserted stereotaxically into the right frontal cerebral white matter. Then, 1.0 ml of autologous arterial blood was injected with an infusion pump at a rate of 100 μl/min. After a 5-min break, another 1.5 ml blood was infused. The catheter was then slowly withdrawn. The burr hole was filled with bone wax and the skin incision was closed with sutures.

2.3. Experimental protocol

This study was in two parts. In the first part, animals were subjected to ICH in the right frontal lobe. Then animals were euthanized at day 1 ($n = 8$), day 3 ($n = 8$), and day 7 ($n = 8$) and brains were harvested for immunohistochemistry, immunofluorescence and hemin assay. Three sham animals only had a needle insertion. In the second part, a total of 32 piglets with ICH model in the frontal lobe were treated with vehicle (saline, $n = 16$) or DFX ($n = 16$) with a dose of 50 mg/kg via intramuscular injection at 2 h after ICH and then every 12 h for up to 7 days. Brains were harvested at day 3 ($n = 8$) and 7 ($n = 8$) for analysis of brain histology ($n = 4$ each group) and hemin assay ($n = 4$ each group).

2.4. Brain in situ freezing and brain histology

The piglets were anesthetized and the brains were frozen in situ by decanting liquid nitrogen into a bottomless foam cup adhered to the head with Dow Corning high vacuum grease (Dow Corning, Midland, MI)(Wagner et al., 1998). The piglets were decapitated and brains were harvested following the injection of potassium chloride to stop the heart beating. Then the frozen head was cut into 5-mm-thick coronal sections by a band saw. Tissues were sampled from the points of interest. For brain histology, the piglets were re-anesthetized and the brains were perfused with 10% formalin. Brains were then sectioned coronally. Paraffin-embedded brain was cut into 10-μm-thick sections and examined with immunohistochemistry and immunofluorescence.

2.5. Hemin assay

For free hemin assay, the brains were in situ frozen. The hematoma and perihematomal white matter tissue samples were collected, weighed, and homogenized as previously described (Wagner et al., 1996). The amount of free hemin was determined by using Hemin Colorimetric Assay kit (Biovision, K672) according to the manufacturer's instructions.

2.6. Immunohistochemistry and cells counting

The 10-μm-thick brain sections were deparaffinized in xylene and rehydrated in a graded series of alcohol dilutions. The microwave boiling method was conducted to retrieve antigen using citrate buffer (10 mmol/L, pH 6.0). Immunohistochemistry examination was performed by avidin-biotin complex techniques(Zheng et al., 2015). The primary antibodies were rabbit monoclonal anti-CD91 (Abcam, ab92544, 1:200 dilution) and rabbit polyclonal anti-Hpx (Abcam, ab133415, 1:400 dilution). Phosphate-buffered saline (0.1 M, pH 7.4) was employed as a negative control. Counting of CD91and Hpx-positive cells was performed on high-power images (×40 magnification) taken using a digital camera. Counts were performed on 4 areas in each brain section.

2.7. Immunofluorescence

For immunofluorescence triple labeling, paraffin-embedded sections were dealt with the same method as described above to retrieve antigen. Then they were treated with 0.3% Triton X-100 in PBS and blocked using normal donkey serum for 30 min at room temperature. The primary antibody incubation was applied for 1.5 h or overnight at 4 °C. Sections were then rinsed with PBS for 10 min 3 times and incubated with secondary antibodies at room temperature for 2 h. The primary antibodies were rabbit monoclonal anti-CD91 (Abcam, ab92544, 1:100 dilution), rabbit polyclonal anti-Hpx (Abcam, ab133415, 1:300 dilution), goat polyclonal anti-Iba1 (1:300, ab107159, Abcam). DAPI was used for nuclear labeling.

2.8. Statistical analysis

Measurements were performed by personnel blinded to each group. All the data are expressed as mean ± SD. Data were compared by using one- or two-way ANOVA with a Bonferroni multiple comparisons test. A probability value of < 0.05 was considered statistically significant. Because these are novel endpoints for a porcine ICH model, we were not able to perform a power analysis to determine sample size. However, in a prior study(Gu et al., 2009), four animals per group was able to detect a 50% reduction in ferritin-positive cells with DFX at the $p < .05$ level.

3. Results

Hemin content in the hematoma and perihematomal brain tissue was measured to assess erythrolysis. Hemin concentrations in the contralateral hemisphere were low (3.3 ± 0.3 μg/g). In contrast, hemin levels in the hematoma were ~500–700 folds higher

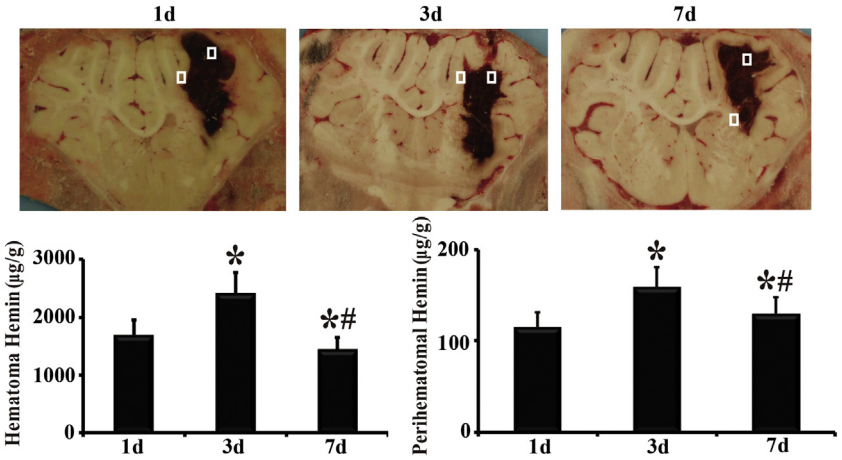

Fig. 1. Hematomal and perihematomal hemin levels at days 1, 3, and 7 following ICH. Sample areas are shown in brain sections. *, $p < .05$, compared with day 1; #, $p < .05$, compared with day 3.

(1693 ± 339 and 2408 ± 474 μg/g at day 1 and 3, respectively) although there was some reduction by day 7 ($p < .05$, Fig. 1). Hemin content in the perihematomal brain tissue was also much higher (35–50 fold) than in the contralateral tissue (e.g. 115 ± 17 μg/g at day 1). Like, hematomal hemin, perihematomal hemin peaked at day 3 (Fig. 1).

Expression of Hpx, the major hemin scavenger, in brain hematoma and perihematomal areas was determined using immunohistochemistry. We found that some Hpx expression in the clot at day 1 (233 ± 86 cells/mm^2) after ICH, then it increased at day 3 and at day 7 (e.g. 645 ± 109 cells/mm^2 at day 7, Fig. 2A). Hpx positive cells in the perihematomal tissue showed a similar time course (Fig. 2B). To further determine what cells expressed Hpx, we performed triple immunofluorescence staining. We found that Hpx was co-localized with Iba1 (a microglia/macrophage marker, Fig. 2C).

The levels of CD91 in the hematoma and perihematomal zone were also determined. Immunohistochemistry showed that CD91-positive cells infiltrated into the hematoma from the edge to center after ICH, with a marked upregulation at day 3 and stayed at high level at day 7 (1224 ± 191 cells/mm^2, Fig. 3A). CD91 expression in the perihematomal zone increased with time ($p < .05$, Fig. 3B). The morphological features of the CD91-positive cells in and around the clot were microglia/macrophage like, which was further confirmed by its co-localization with Iba1 using immunofluorescence (Fig. 3C).

To determine whether DFX affects hemin release and clearance, ICH rats were treated with vehicle or DFX for up to 7 days. Our results showed that hemin content in the hematoma was significantly lower in the DFX-treated group than in the vehicle-treated group at both day 3 and day 7 ($p < .05$, Fig. 4). The same phenomena happened in the perihematomal brain ($p < .05$, Fig. 4). Whether DFX produces an effect on Hpx and CD91 expression was further investigated. Hpx levels in

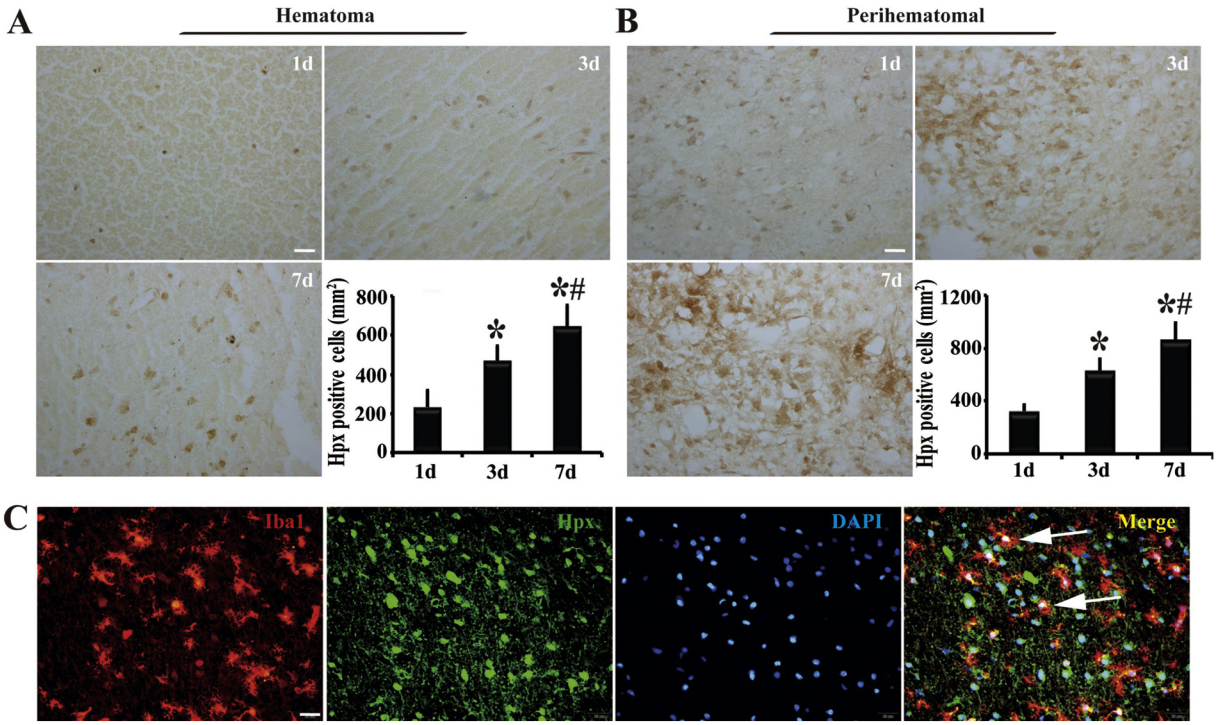

Fig. 2. Presence of hemopexin (Hpx)-positive cells in (A) hematoma and (B) perihematomal tissue at days 1, 3 and 7 after ICH with quantification. Scale bar = 20 μm. $n = 4$ for each group, *, $p < .05$, compared with day 1; #, $p < .05$, compared with day 3. (C) At day 1 after ICH, Hpx immunoreactivity colocalized with Iba1 in the perihematomal area. Arrows indicate double-stained cells. Scale bar = 20 μm.

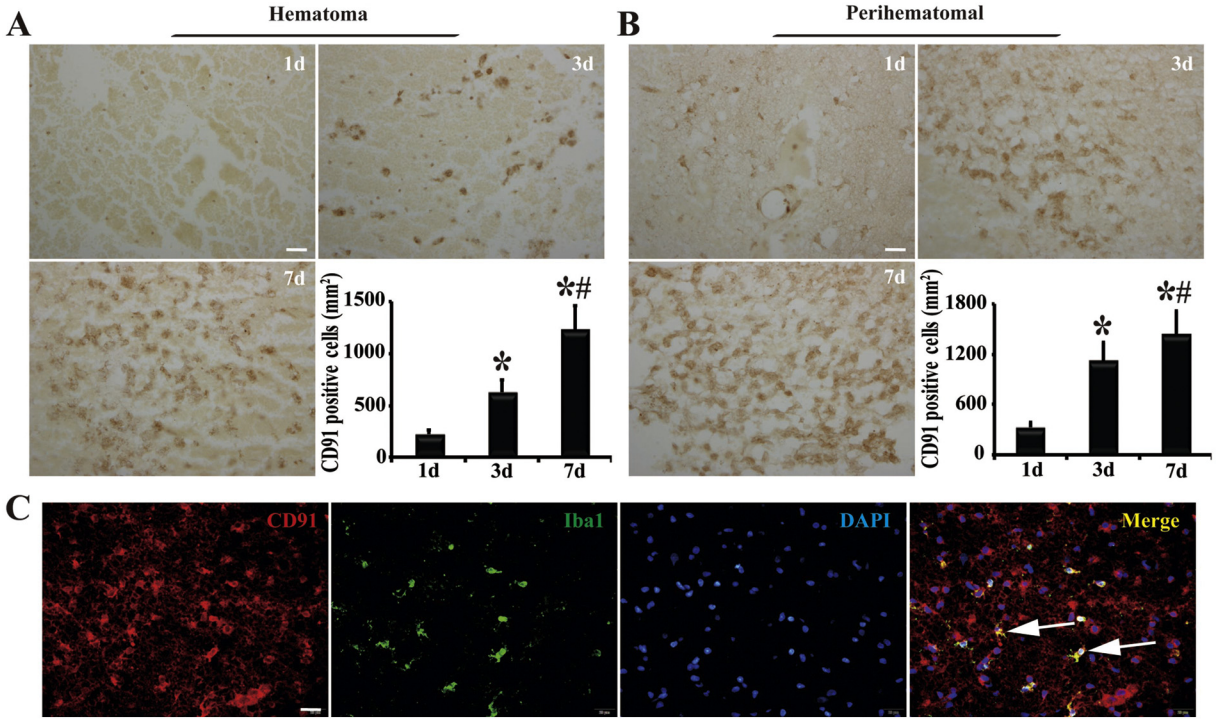

Fig. 3. Presence of CD91-positive cells in (A) clot and (B) perihematomal tissue 1, 3 and 7 days after ICH with quantification. Scale bar = 20 μm. $n = 4$ for each group, *, $p < .05$, compared with day 1; #, $p < .05$, compared with day 3. (C) CD91-immunoreactivity colocalized with Iba1 in the perihematomal area at day 1. Scale bar = 20 μm. Arrows indicate double-stained cells.

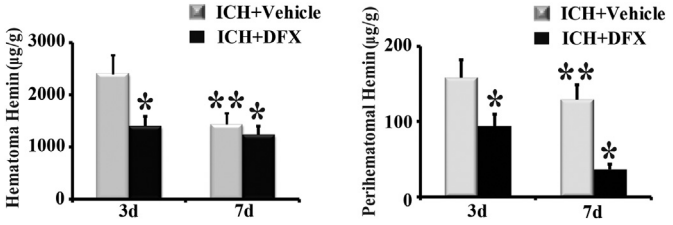

Fig. 4. Deferoxamine (DFX) treatment reduced hemin levels in (A) hematoma and (B) perihematomal tissue at day 3 and 7 following ICH. $n = 4$ for each group. * $p < .05$, compared with the vehicle-treated group; ** $p < .05$ compared with day 3.

the hematoma and perihematomal zone declined significantly after DFX therapy at day 7 ($p < .01$, Fig. 5). Additionally, DFX treatment reduced CD91-positive cells in the clot and perihematomal tissue at day 7 ($p < .01$, Fig. 6).

4. Discussion

The major findings in the current study are: (Mendelow et al., 2013) hemin concentrations in hematoma and perihematomal tissue are markedly elevated compared to normal brain, (Keep et al., 2012) those hemin levels can be reduced by DFX treatment; (Selim and Sheth, 2015) expression of Hpx in the clot and perihematomal tissue occurs at day 1 after ICH and increases with time; (Schlunk and Greenberg, 2015) there is a progressive increase of CD91-positive cells in hematoma and perihematomal brain tissue; (Wilkinson et al., 2018) DFX down regulates Hpx and CD91 in clot and perihematomal brain tissue. These data suggest that hemin release hematoma occurs from the first day following ICH and that there is a compensatory activation of the hemin scavenger systems (Fig. 7). DFX reduces hemin release and, thus, ICH-induced upregulation of Hpx and CD91.

Hematoma resolution after ICH still remains a relatively understudied area. It may involve the phagocytosis of the hematoma by microglia/macrophages and erythrocyte lysis with the clearance of the products of such lysis, particularly hemoglobin and its degradation products(Wan et al., 2016; Xiong and Yang, 2015; Zhao et al., 2015). The latter include hemin and iron that are potentially neurotoxic (Keep et al., 2012; Xi et al., 2006). To examine the progress of erythrocyte lysis after ICH, the current study measured hemin levels within the hematoma and in perihematomal brain. Very high hemin levels were recorded within the hematoma after ICH (~2000 μg/g or approximately 3 mM) and in perihematomal tissue (~130 μg/g or approximately 0.2 mM). We have recently reported a progressive decrease in hematoma hemoglobin content (determined by ELISA) over the first three days in this piglet ICH model (Cao et al., 2016) that mirrors the increase in hemin. The increase in perihematomal hemin after ICH in the current study probably reflects diffusion of the hematomal hemin into the surrounding tissue. The hemin assay used in the current study uses the peroxidase activity of hemin. Such activity is reduced by hemopexin binding(Schaer et al., 2013) and it is possible that tissue processing may have affected such binding. There is a need to determine free hemin concentrations in vivo, particularly in the extracellular space.

The release of hemin after erythrolysis may contribute to ICH-induced brain injury (Robinson et al., 2009; Babu et al., 2012; Garton et al., 2016; Keep et al., 2018). Thus, for example, direct intracaudate injection of hemin causes brain edema in the rat (Huang et al., 2002) and, in vitro, 50 μM hemin induces neuronal cell death (Karuppagounder et al., 2016). In this study, our measured brain tissue hemin concentrations adjacent to the hematoma (~200 μM) are greater than those required to cause neuronal death in vitro.

The current study showing increased hematomal and perihematomal hemin concentrations by as early as one day, supports growing evidence that some erythrocyte lysis occurs early after ICH. As noted above, we have found a progressive loss of hemoglobin in the hematoma over 3 days in the same piglet ICH model(Cao et al., 2016). T_2^* magnetic resonance imaging of the brain at day 1 also showed hyperintense signals in the center of hematoma which may represents the

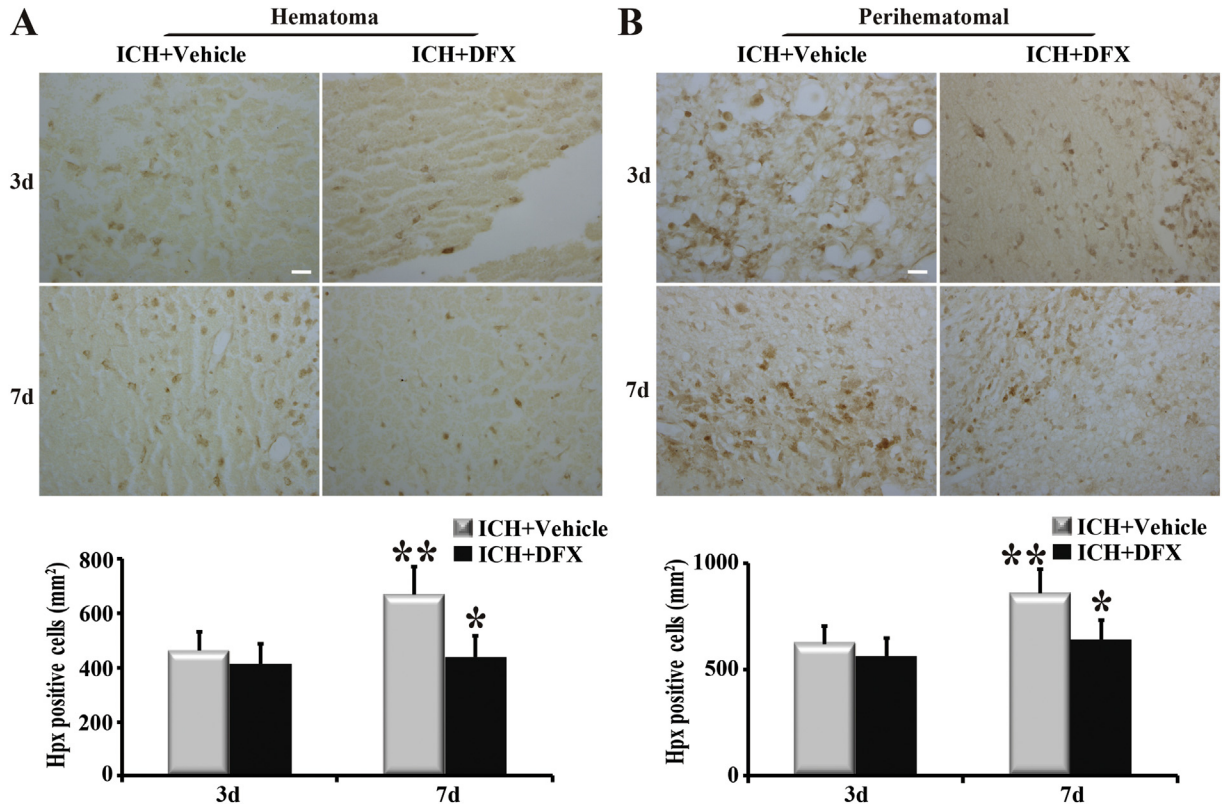

Fig. 5. Deferoxamine (DFX) treatment down regulated the expression of hemopexin (Hpx) in (A) clot and (B) perihematomal tissue at day 7 following ICH. Examples of Hpx immunohistochemistry at days 3 and 7 after ICH. Scale bar = 20 μm. Quantification of the numbers of Hpx immunopositive cells with and without DFX treatment. $n = 4$ for each group. * $p < .01$, compared to vehicle-treated group; ** $p < .05$ compared with day 3.

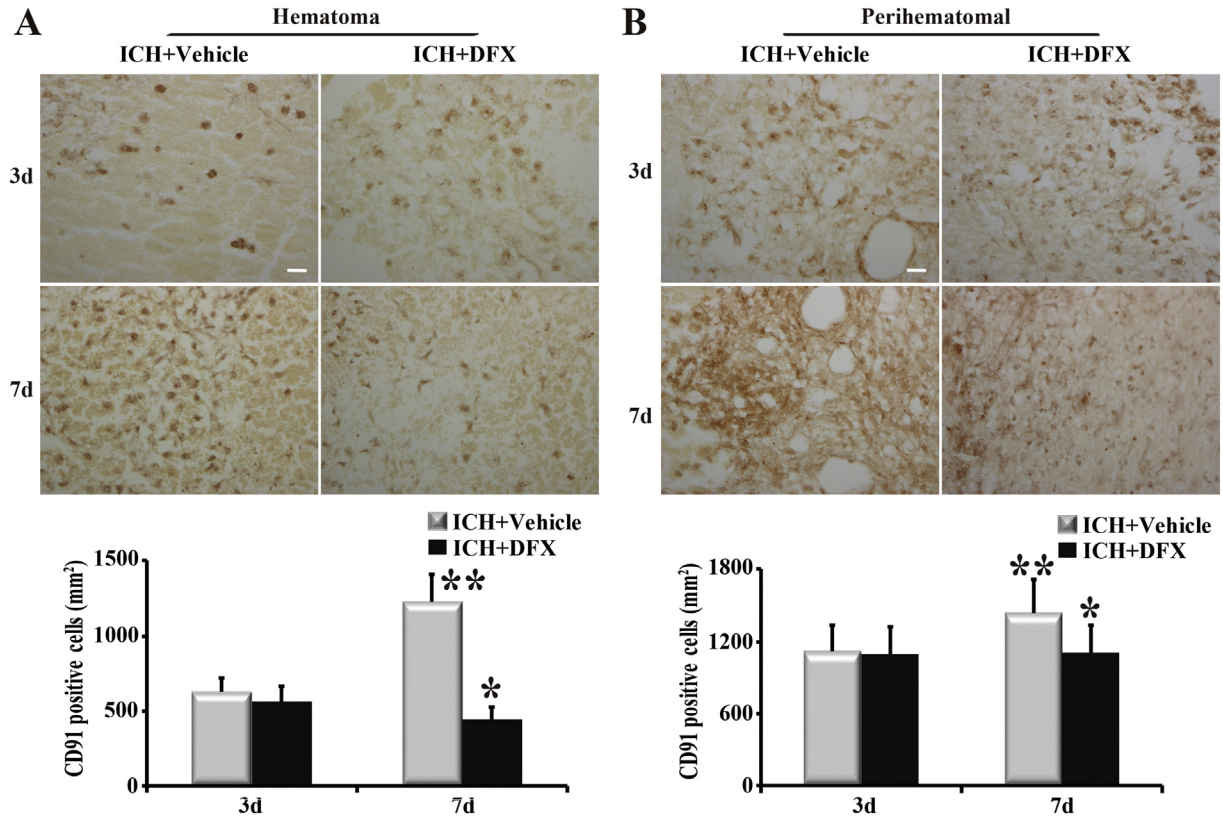

Fig. 6. Deferoxamine (DFX) treatment decreased the expression of CD91 in (A) the hematoma and (B) perihematomal tissue at day 7. Examples of CD91 immunohistochemistry at days 3 and 7 after ICH; scale bar = 20 μm. Quantification of the numbers of CD91 immunopositive cells with and without DFX treatment. $n = 4$ for each group. * $p < .05$ compared to vehicle-treated group; ** $p < .05$ compared with day 3.

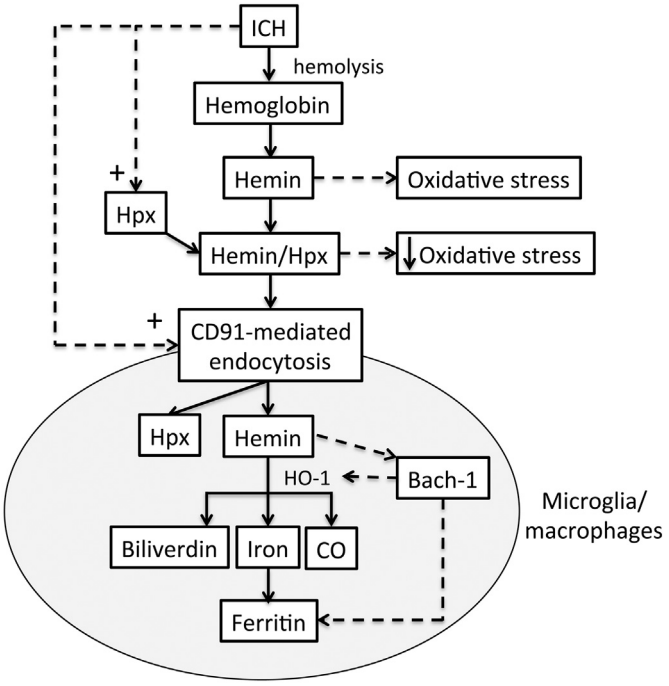

Fig. 7. Schematic for hemin clearance by microglia/macrophages following ICH. Hemolysis after ICH causes the release of hemoglobin and hemin. The oxidative stress that can be caused by hemin is reduced by binding to hemopexin (Hpx) which is upregulated after ICH as shown by the current study. In addition, the hemin/Hpx complex is taken up into microglia/macrophages via CD91-mediated endocytosis. CD91 is also upregulated in brain after ICH as shown in the current study. Within microglia/macrophages, hemin is degraded into iron, carbon monoxide (CO) and bilverdin by heme oxygenase-1 (HO-1). Iron is chelated by ferritin to prevent iron-induced oxidative stress. Both HO-1 and ferritin are upregulated after ICH. Hemin increasing their expression by binding to Bach-1, a transcription factor that normally represses the expression of these proteins.

early erythrocyte lysis with the appearance of erythrocyte ghosts on histology(Dang et al., 2017). In line with these data, hemoglobin was present in the perihematomal zone at day 1 after ICH in a rabbit model (Koeppen et al., 1995). The time course of hemoglobin, hemin and iron release after ICH is important because there is an upregulation of various mechanisms in brain after ICH that may limit hemoglobin, hemin and iron toxicity (Wu et al., 2003). Hemoglobin, hemin and iron release prior to those protective changes may cause more brain injury.

The adverse effects of hemin may be limited by upregulation in Hpx and CD91. Hpx is a 60-kDa serum glycoprotein, which is recognized as the first line of defense system against free hemin. It binds hemin with very high affinity, serving a protective function through limiting the toxic effects of hemin (Chen et al., 2011) including limiting hemin peroxidase activity (Robinson et al., 2009; Schaer et al., 2013). The hemin-Hpx complex can also be taken up by cells via CD91 receptor, and the hemin is then catabolized by the heme oxygenases (Fig. 7) (Kumar and Bandyopadhyay, 2005; Piccard et al., 2007). In present study, we found that Hpx was positive in the hematoma and perihematomal brain tissue at day 1 after ICH and Hpx expression progressively increased with time. Furthermore, our results showed that Hpx-positive cells were also Iba1 positive, which indicated that they were primarily microglia/macrophages. This might be endogenous protective mechanism in response to increased hemin content level with microglia/macrophages being activated and releasing Hpx after ICH to clear hemin. Multiple studies have shown that Hpx has a protective role in the central nervous system and systemic organs (Ma et al., 2016; Dong et al., 2013; Chen et al., 2011; Li et al., 2009; Vinchi et al., 2013; Vinchi et al., 2016; Lin et al., 2016; Deuel et al., 2015; Hahl et al., 2013).

CD91 is a transmembrane receptor that is expressed on several types of brain cell, including microglia/macrophages. Amongst several functions, it is involved in the endocytosis of the hemin/Hpx complex (Robinson et al., 2009; Hvidberg et al., 2005). In our experiments, there was a progressive increase in CD91 expression after ICH both within the clot and in the perihematomal tissue, where CD91 colocalized with Iba-1, a microglial marker. While further studies are needed to explore whether CD91 upregulation on microglia/macrophages is beneficial in ICH, it may represent a method for clearing extracellular hemin.

Both Hpx and CD91 showed a progressive increase in expression after ICH. The mechanism involved in that upregulation is still uncertain and needs to be investigated. It is known that hemin is involved in the upregulation of HO-1 and ferritin by binding to Bach-1, a transcription factor that normally suppresses the transcription of those proteins (Hada et al., 2014) (Fig. 7) but whether hemin, or some other clot-derived factor, induces the upregulation of Hpx and CD91 after ICH is uncertain. As with ferritin (Wu et al., 2003), the increase in Hpx and CD91 is delayed after ICH. Whether this means that early release (e.g. in the first day) of hemin after ICH causes more brain injury than later release needs to be investigated as does the role of heme carrier protein 1 (HCP1) that may also be involved in hemin clearance (Robinson et al., 2009).

Our prior studies have shown that DFX reduces ICH-induced brain injury in mice, rats and pigs(Keep et al., 2012; Xi et al., 2006) and DFX is currently in phase II clinical trial for ICH (NCT02175225). DFX is an iron chelator and perihematomal iron overload occurs after ICH (Wu et al., 2003) and much evidence indicates iron is involved in ICH-induced brain injury (Keep et al., 2012; Xi et al., 2006). The current study also indicates that DFX also reduces erythrolysis and the release of hemin within the hematoma and into perihematomal tissue. This work confirms a prior study demonstrating that DFX slowed erythrolysis and the release of hemoglobin from the hematoma (Cao et al., 2016). Thus, DFX may reduce ICH-induced brain injury by multiple mechanisms as well as iron chelation, including delaying the release of potential neurotoxic compounds (hemin and hemoglobin) from the hematoma by inhibiting erythrolysis. Interestingly, DFX also decreased the number of Hpx and CD91-positive cells in both clot and perihematomal area. This may be the result of the reduced erythrolysis and lower levels of the clot-derived factor that induces Hpx and CD91 expression.

5. Conclusions

In summary, this study presents data on the natural changes of hemin-hemopexin-CD91 axis in a large animal ICH model. DFX treatment reduces hemin levels in and around the hematoma. Enhancing hemin clearance may reduce ICH-induced brain injury.

Funding

YH, RFK and GX were supported by grants NS-091545, NS-090925, NS-096917 and NS-106746 from the National Institutes of Health (NIH).

Conflict of interests

Shengli Hu, Ya Hua, Richard F. Keep, Hua Feng and Guohua Xi declare no conflict of interests.

Ethical approval

All institutional and national guidelines for the care and use of laboratory animals were followed.

References

Aronowski, J., Zhao, X., 2011. Molecular pathophysiology of cerebral hemorrhage: secondary brain injury. Stroke 42 (6), 1781–1786 Jun. PubMed PMID: 21527759. Pubmed Central PMCID: 3123894. Epub 2011/04/30. eng.

Ascenzi, P., Bocedi, A., Visca, P., Altruda, F., Tolosano, E., Beringhelli, T., et al., 2005. Hemoglobin and heme scavenging. IUBMB Life 57 (11), 749–759 Nov. PubMed PMID: 16511968.

Babu, R., Bagley, J.H., Di, C., Friedman, A.H., Adamson, C., 2012. Thrombin and hemin as central factors in the mechanisms of intracerebral hemorrhage-induced secondary brain injury and as potential targets for intervention. Neurosurg. Focus. 32 (4), E8 Apr. PubMed PMID: 22463118.

Cao, S., Zheng, M., Hua, Y., Chen, G., Keep, R.F., Xi, G., 2016. Hematoma changes during clot resolution after experimental intracerebral hemorrhage. Stroke. 47, 1626–1631 Apr 28. PubMed PMID: 27125525. Epub 2016/04/30. Eng.

Chen, L., Zhang, X., Chen-Roetling, J., Regan, R.F., 2011. Increased striatal injury and behavioral deficits after intracerebral hemorrhage in hemopexin knockout mice. J. Neurosurg. 114 (4), 1159–1167 Apr. PubMed PMID: 21128737. Pubmed Central PMCID: 3061252. Epub 2010/12/07. eng.

Dang, G., Yang, Y., Wu, G., Hua, Y., Keep, R.F., Xi, G., 2017. Early erythrolysis in the hematoma after experimental intracerebral hemorrhage. Transl. Stroke Res. 8, 174–182 Oct 25. PubMed PMID: 27783383. Epub 2016/10/27. eng.

Deuel, J.W., Vallelian, F., Schaer, C.A., Puglia, M., Buehler, P.W., Schaer, D.J., 2015. Different target specificities of haptoglobin and hemopexin define a sequential protection system against vascular hemoglobin toxicity. Free Radic. Biol. Med. 89, 931–943 Dec. PubMed PMID: 26475040. Epub 2015/10/18. eng.

Dong, B., Cai, M., Fang, Z., Wei, H., Zhu, F., Li, G., et al., 2013. Hemopexin induces neuroprotection in the rat subjected to focal cerebral ischemia. BMC Neurosci. 14, 58 PubMed PMID: 23758755. Pubmed Central PMCID: 3694464. Epub 2013/06/14. eng.

Garton, T., Keep, R.F., Wilkinson, D.A., Strahle, J.M., Hua, Y., Garton, H.J., et al., 2016. Intraventricular hemorrhage: the role of blood components in secondary injury and hydrocephalus. Transl. Stroke Res. 7, 447–451 Jun 30. PubMed PMID: 27358176.

Gu, Y., Hua, Y., Keep, R.F., Morgenstern, L.B., Xi, G., 2009. Deferoxamine reduces intracerebral hematoma-induced iron accumulation and neuronal death in piglets. Stroke 40 (6), 2241–2243 Jun. PubMed PMID: 19372448. Epub 2009/04/18. eng.

Hada, H., Shiraki, T., Watanabe-Matsui, M., Igarashi, K., 2014. Hemopexin-dependent heme uptake via endocytosis regulates the Bach1 transcription repressor and heme oxygenase gene activation. Biochim. Biophys. Acta 1840 (7), 2351–2360 Jul. PubMed PMID: 24613679. Epub 2014/03/13. eng.

Hahl, P., Davis, T., Washburn, C., Rogers, J.T., Smith, A., 2013. Mechanisms of neuroprotection by hemopexin: modeling the control of heme and iron homeostasis in brain neurons in inflammatory states. J. Neurochem. 125 (1), 89–101 Apr. PubMed PMID: 23350672. Pubmed Central PMCID: 3752430. Epub 2013/01/29. eng.

Hatakeyama, T., Okauchi, M., Hua, Y., Keep, R.F., Xi, G., 2013. Deferoxamine reduces neuronal death and hematoma lysis after intracerebral hemorrhage in aged rats. Transl. Stroke Res. 4 (5), 546–553 Oct. PubMed PMID: 24187595. Pubmed Central PMCID: 3810989.

Huang, F.P., Xi, G., Keep, R.F., Hua, Y., Nemoianu, A., Hoff, J.T., 2002. Brain edema after experimental intracerebral hemorrhage: role of hemoglobin degradation products. J. Neurosurg. 96 (2), 287–293 Feb. PubMed PMID: 11838803. Epub 2002/02/13. eng.

Hvidberg, V., Maniecki, M.B., Jacobsen, C., Hojrup, P., Moller, H.J., Moestrup, S.K., 2005. Identification of the receptor scavenging hemopexin-heme complexes. Blood 106 (7), 2572–2579 Oct 1. PubMed PMID: 15947085. Epub 2005/06/11. eng.

Karuppagounder, S.S., Alim, I., Khim, S.J., Bourassa, M.W., Sleiman, S.F., John, R., et al., 2016. Therapeutic targeting of oxygen-sensing prolyl hydroxylases abrogates ATF4-dependent neuronal death and improves outcomes after brain hemorrhage in several rodent models. Sci. Transl. Med. 8 (328), 328ra29 Mar 2. PubMed PMID: 26936506.

Keep, R.F., Hua, Y., Xi, G., 2012. Intracerebral haemorrhage: mechanisms of injury and therapeutic targets. Lancet Neurol. 11 (8), 720–731 Aug. PubMed PMID: 22698888. Pubmed Central PMCID: 3884550. Epub 2012/06/16. eng.

Keep, R.F., Andjelkovic, A.V., Xiang, J., Stamatovic, S.M., Antonetti, D.A., Hua, Y., et al., 2018. Brain endothelial cell junctions after cerebral hemorrhage: changes, mechanisms and therapeutic targets. J. Cereb. Blood Flow Metab. 38 (8), 1255–1275 Aug. PubMed PMID: 29737222. Pubmed Central PMCID: 6092767.

Koeppen, A.H., Dickson, A.C., McEvoy, J.A., 1995. The cellular reactions to experimental intracerebral hemorrhage. J. Neurol. Sci. 134, 102–112.

Kumar, S., Bandyopadhyay, U., 2005. Free heme toxicity and its detoxification systems in human. Toxicol. Lett. 157 (3), 175–188 Jul 4. PubMed PMID: 15917143. Epub 2005/05/27. eng.

Li, R.C., Saleem, S., Zhen, G., Cao, W., Zhuang, H., Lee, J., et al., 2009. Heme-hemopexin complex attenuates neuronal cell death and stroke damage. J. Cereb. Blood Flow Metab. 29 (5), 953–964 May. PubMed PMID: 19277051. Epub 2009/03/12. eng.

Lillis, A.P., Van Duyn, L.B., Murphy-Ullrich, J.E., Strickland, D.K., 2008. LDL receptor-related protein 1: unique tissue-specific functions revealed by selective gene knockout studies. Physiol. Rev. 88 (3), 887–918 Jul. PubMed PMID: 18626063. Pubmed Central PMCID: 2744109. Epub 2008/07/16. eng.

Lin, T., Liu, J., Huang, F., Van Engelen, T.S., Thundivalappil, S.R., Riley, F.E., et al., 2016. Purified and recombinant hemopexin: protease activity and effect on neutrophil chemotaxis. Mol. Med. 22, 22–31 Jan 8. PubMed PMID: 26772775. Pubmed Central PMCID: 5004720. Epub 2016/01/17. Eng.

Ma, B., Day, J.P., Phillips, H., Slootsky, B., Tolosano, E., Dore, S., 2016. Deletion of the hemopexin or heme oxygenase-2 gene aggravates brain injury following stroma-free hemoglobin-induced intracerebral hemorrhage. J. Neuroinflammation 13 26. PubMed PMID: 26831741. Pubmed Central PMCID: 4736638. Epub 2016/02/03. eng.

Mendelow, A.D., Gregson, B.A., Rowan, E.N., Murray, G.D., Gholkar, A., Mitchell, P.M., et al., 2013. Early surgery versus initial conservative treatment in patients with spontaneous supratentorial lobar intracerebral haematomas (STICH II): a randomised trial. Lancet 382 (9890), 397–408 Aug 3. PubMed PMID: 23726393. Pubmed Central PMCID: 3906609.

Piccard, H., Van den Steen, P.E., Opdenakker, G., 2007. Hemopexin domains as multifunctional liganding modules in matrix metalloproteinases and other proteins. J. Leukoc. Biol. 81 (4), 870–892 Apr. PubMed PMID: 17185359. Epub 2006/12/23. eng.

Ramanathan, A., Nelson, A.R., Sagare, A.P., Zlokovic, B.V., 2015. Impaired vascular-mediated clearance of brain amyloid beta in Alzheimer's disease: the role, regulation and restoration of LRP1. Front. Aging Neurosci. 7, 136 PubMed PMID: 26236233. Pubmed Central PMCID: 4502358. Epub 2015/08/04. eng.

Robinson, S.R., Dang, T.N., Dringen, R., Bishop, G.M., 2009. Hemin toxicity: a preventable source of brain damage following hemorrhagic stroke. Redox Rep.: Commun. Free Rad. Res. 14 (6), 228–235 PubMed PMID: 20003707.

Schaer, D.J., Buehler, P.W., Alayash, A.I., Belcher, J.D., Vercellotti, G.M., 2013. Hemolysis and free hemoglobin revisited: exploring hemoglobin and hemin scavengers as a novel class of therapeutic proteins. Blood 121 (8), 1276–1284 Feb 21. PubMed PMID: 23264591. Pubmed Central PMCID: 3578950. Epub 2012/12/25. eng.

Schlunk, F., Greenberg, S.M., 2015. The pathophysiology of intracerebral hemorrhage formation and expansion. Transl. Stroke Res. 6 (4), 257–263 Aug. PubMed PMID: 26073700.

Selim, M., Sheth, K.N., 2015. Perihematoma edema: a potential translational target in intracerebral hemorrhage? Transl. Stroke Res. 6 (2), 104–106 Apr. PubMed PMID: 25693976. Pubmed Central PMCID: 4359064.

Soares, M.P., Bozza, M.T., 2016. Red alert: labile heme is an alarmin. Curr. Opin. Immunol. 38, 94–100 Feb. PubMed PMID: 26741528. Epub 2016/01/08. eng.

Vinchi, F., De Franceschi, L., Ghigo, A., Townes, T., Cimino, J., Silengo, L., et al., 2013. Hemopexin therapy improves cardiovascular function by preventing heme-induced endothelial toxicity in mouse models of hemolytic diseases. Circulation 127 (12), 1317–1329 Mar 26. PubMed PMID: 23446829. Epub 2013/03/01. eng.

Vinchi, F., Costa da Silva, M., Ingoglia, G., Petrillo, S., Brinkman, N., Zuercher, A., et al., 2016. Hemopexin therapy reverts heme-induced proinflammatory phenotypic switching of macrophages in a mouse model of sickle cell disease. Blood 127 (4), 473–486 Jan 28. PubMed PMID: 26675351. Pubmed Central PMCID: 4850229. Epub 2015/12/18. eng.

Wagener, F.A., Eggert, A., Boerman, O.C., Oyen, W.J., Verhofstad, A., Abraham, N.G., et al., 2001. Heme is a potent inducer of inflammation in mice and is counteracted by heme oxygenase. Blood 98 (6), 1802–1811 Sep 15. PubMed PMID: 11535514. Epub 2001/09/06. eng.

Wagner, K.R., Xi, G., Hua, Y., Kleinholz, M., de Courten-Myers, G.M., Myers, R.E., et al., 1996. Lobar intracerebral hemorrhage model in pigs: rapid edema development in perihematomal white matter. Stroke 27 (3), 490–497.

Wagner, K.R., Xi, G., Hua, Y., Kleinholz, M., de Courten-Myers, G.M., Myers, R.E., 1998. Early metabolic alterations in edematous perihematomal brain regions following experimental intracerebral hemorrhage. J. Neurosurg. 88 (6), 1058–1065.

Wan, S., Cheng, Y., Jin, H., Guo, D., Hua, Y., Keep, R.F., et al., 2016. Microglia activation and polarization after intracerebral hemorrhage in mice: the role of protease-activated receptor-1. Transl. Stroke Res. 7, 478–487 May 21. PubMed PMID: 27206851.

Wang, G., Manaenko, A., Shao, A., Ou, Y., Yang, P., Budbazar, E., et al., 2016. Low-density lipoprotein receptor-related protein-1 facilitates heme scavenging after intracerebral hemorrhage in mice. J. Cereb. Blood Flow Metab. 37 (4), 1299–1310. https://doi.org/10.1177/0271678X16654494. Jun 17. PubMed PMID: 27317656. Epub 2016/06/19. Eng.

Wilkinson, D.A., Keep, R.F., Hua, Y., Xi, G., 2018. Hematoma clearance as a therapeutic target in intracerebral hemorrhage: from macro to micro. J. Cereb. Blood Flow Metab. 38 (4), 741–745 Apr. PubMed PMID: 29350086. Pubmed Central PMCID: 5888862.

Wu, J., Hua, Y., Keep, R.F., Nakamura, T., Hoff, J.T., Xi, G., 2003. Iron and iron-handling proteins in the brain after intracerebral hemorrhage. Stroke 34 (12), 2964–2969.

Xi, G., Keep, R.F., Hoff, J.T., 2006. Mechanisms of brain injury after intracerebral haemorrhage. Lancet Neurol. 5 (1), 53–63 Jan. PubMed PMID: 16361023. Epub 2005/12/20. eng.

Xie Q, Gu Y, Hua Y, Liu W, Keep RF, Xi G. Deferoxamine attenuates white matter injury in a piglet intracerebral hemorrhage model. Stroke. 2014 Jan;45(1):290–2. PubMed PMID: 24172580. Pubmed Central PMCID: 3886635.

Xiong, X.Y., Yang, Q.W., 2015. Rethinking the roles of inflammation in the intracerebral hemorrhage. Transl. Stroke Res. 6 (5), 339–341 Oct. PubMed PMID: 25940771.

Zhao, H., Garton, T., Keep, R.F., Hua, Y., Xi, G., 2015. Microglia/macrophage polarization after experimental intracerebral hemorrhage. Transl. Stroke Res. 6 (6), 407–409 Dec. PubMed PMID: 26446073. Pubmed Central PMCID: 4628553.

Zheng, M., Du, H., Ni, W., Koch, L.G., Britton, S.L., Keep, R.F., et al., 2015. Iron-induced necrotic brain cell death in rats with different aerobic capacity. Transl. Stroke Res. 6 (3), 215–223 Jun. PubMed PMID: 25649272. Pubmed Central PMCID: 4425582.

Zhou, X., Xie, Q., Xi, G., Keep, R.F., Hua, Y., 2014. Brain CD47 expression in a swine model of intracerebral hemorrhage. Brain Res. 1574, 70–76 Jul 29. PubMed PMID: 24931767.